

Selective production of light olefins from methanol over desilicated highly siliceous ZSM-5 nanocatalysts

Mohammad Rostamizadeh^{*1,2}, Fereydoon Yaripour³, Hossein Hazrati^{1,2}

¹Department of Chemical Engineering, Sahand University of Technology, Sahand New Town, Tabriz, Iran

²Environmental Engineering Research Center, Sahand University of Technology, Sahand New Town, Tabriz, Iran

³Catalysis Research Group, Petrochemical Research & Technology Company, National Iranian Petrochemical Company, Tehran, Iran

Received: 17 July 2017, Accepted: 3 September 2017

ABSTRACT

Highly siliceous ZSM-5 nanocatalysts can dehydrate methanol to a wide range of hydrocarbons. In this study, the development of hierarchical H-ZSM-5 nanocatalysts (Si/Al=200) were reported for the methanol-to-olefins (MTO) reaction. The nanocatalysts were prepared through a hydrothermal technique and treated by NaOH desilication. The parent and desilicated nanocatalysts were characterized using FE-SEM, XRD, FTIR, NH₃-TPD and N₂ adsorption-desorption techniques. The mesoporosity increased five times without significant collapse of the crystalline framework as a result of the appropriate desilication of H-ZSM-5 nanocatalyst. For the nanocatalyst, a high surface area of 189.5 m² g⁻¹, mesopore volume of 0.35 cm³ g⁻¹ and well-adjusted strong acidity of 0.16 mmol NH₃ g⁻¹ resulted in a high methanol conversion of 100%, high propylene selectivity of 43% and low light paraffins selectivity of <8% in the MTO reaction. A broad mesopore size of 2-10 nm suppressed coke deposition and provided a long catalytic life time of 75 h. The developed high silica nanocatalyst showed a high potential for industrial applications due to its stable performance. **Polyolefins J (2017) 5: 59-70**

Keywords: Hierarchical zeolites; ZSM-5; desilication; nanocatalyst, MTO.

INTRODUCTION

Among petrochemical products, light olefins (ethylene and propylene) are highly demanded [1]. The current processes including steam cracking and fluid catalytic cracking (FCC) technologies are greatly energy consuming, low olefin yield and oil-dependent feed stock. The shortage of fossil fuel sources, continuously growing oil price and availability of huge natural gas resources have been led to try to find new routes for olefin production. Natural gas, biomass and coal as carbon sources can be converted to the synthesis gas

which, in turn, can be used for producing methanol [2, 3]. Acidic zeolite catalysts dehydrate methanol to a wide range of hydrocarbons. The product distribution in the methanol to olefins (MTO) reaction strongly depends on the catalyst type [4-7]. In general, olefin selectivity and catalytic lifetime are the main issues in the MTO catalyst development, which highlights the necessity of catalyst modification. Among catalyst properties, the acidity and textural specification of catalyst play a key role in the MTO reaction. Desilication treatment extracts silicon species from the zeolite structure, which results in acidity and pore size modification. In preparation

* Corresponding Author - E-mail: Rostamizadeh.m@gmail.com, Rostamizadeh@sut.ac.ir

of a hierarchical catalyst several parameters, for example, type of zeolite, Si/Al ratio, and operational conditions influence its performance [8-11]. Fathi et al. [12] modified ZSM-5 (Si/Al=15) catalyst by alkaline treatment (CaCO_3 , Na_2CO_3 and NaOH solution) at 75°C for 3 h and evaluated its properties for using in the methanol to gasoline (MTG) reaction. They found that NaOH treatment (0.1 M) reduced the acidity and created mesoporous structure more than other solutions. The sample treated by Na_2CO_3 provided the highest C_{5+} cut yield (ca. 43 %) and the longest catalytic lifetime (4 h). Ahn et al. [13] tuned diffusion and acid sites concentration of H-ZSM-5 catalyst (Si/Al=36) for the methylation of toluene. They applied 0.2 M NaOH solution at 67°C under stirring for 0.75 h. The treatment increased the surface area ($482\text{ m}^2\text{ g}^{-1}$), mesopore volume ($0.05\text{ cm}^3\text{ g}^{-1}$) and total acidity ($537\text{ pyridine }\mu\text{mol g}^{-1}$). Desilication decreased effective diffusion length which led to the high toluene turnover rate. Yingping et al. [14] studied desilication of ZSM-5 (Si/Al=13) by tetrapropyl ammonium hydroxide (TPAOH) solution (0.1 mol L^{-1}) for different treatment durations (24, 48 and 72 h) at 170°C . The modification increased the surface area, mesopore volume and total acidity, which resulted in the lifetime increasing (170 h) in the MTG reaction.

Ghavipour et al. [15] reported the desilication of H-ZSM-5 catalyst (Si/Al=19) with 0.2 M NaOH solution at 80°C for 3 h. The treated catalyst represented the high methanol conversion (ca. 98 %) and propylene selectivity of ca. 19.3 % after 6 h time on stream. Bleken et al. [16] studied the effect of desilication on the deactivation of H-ZSM-5 (Si/Al=50) catalyst through the methanol to hydrocarbon (MTH) reaction. The catalyst was treated with 0.3 M NaOH solution ($33\text{ cm}^3\text{ g}^{-1}$) for 30 min at 70°C . They found that the desilicated catalyst included more external coke than the parent sample, which could be explained by the lower diffusion resistance and faster hydrocarbon exit. Kim et al. [17] prepared mesopore MFI zeolite catalyst (Si/Al=25) using 0.2 M NaOH solution at 60°C for 30 min and applied for the MTO reaction. The modified catalyst included the high surface area ($402\text{ m}^2\text{ g}^{-1}$) and mesopore volume ($0.19\text{ cm}^3\text{ g}^{-1}$). The desilication increased the catalytic lifetime up to 80 h due to facile diffusion of coke precursors from the micropores to the external surface. They concluded a roughly linear correlation between the mesoporosity and H-ZSM-5 catalytic lifetime in the MTO reaction. Mochizuki et al. [18] studied the desilication of H-ZSM-5 (Si/Al=50) by alkaline treatment (0.05, 0.1 and 0.2 M

NaOH) at 80°C for 1-5 h and characterized in hexane cracking. The high NaOH concentration provided the high surface area ($520\text{ m}^2\text{ g}^{-1}$) and less acid concentration ($0.34\text{ mmol NH}_3\text{ g}^{-1}$). Schmidt et al. [19] synthesized hierarchical ZSM-5 zeolites (Si/Al=50, 140 and 300) by alkaline desilication including N,N,N-trimethylhexadecylammonium bromide (CTAB) as surfactant. 0.5 M NaOH solution including 0.05 M CTAB resulted in the high surface area ($663\text{ m}^2\text{ g}^{-1}$) and total pore volume ($0.7\text{ cm}^3\text{ g}^{-1}$). The treatment increased the catalytic life time up to 100 h including the maximum propylene selectivity of ca. 27 % in the MTO reaction. It is reported that the desilication of ZSM-5 depends on treatment temperature, alkaline solution concentration and time [8, 20, 21].

Only a few research has been performed on the desilication of high silica H-ZSM-5 catalyst and its application for the MTO reaction. However, it is accepted that the mentioned catalyst represents the best performance including the high methanol conversion and olefin selectivity [10, 22, 23]. Consequently, development of an appropriate desilication treatment for the high silica H-ZSM-5 nanocatalyst favors development of an appropriate MTO catalyst. In this study, the main aim was to adjust the acidity and textural properties of high silica H-ZSM-5 nanocatalyst for the MTO reaction through desilication. The appropriate desilication conditions provided a hierarchical nanocatalyst with the high mesoporosity, the less framework destruction and the improved catalytic performance.

EXPERIMENTAL

Materials

All the reagents, including silicic acid ($\text{SiO}_2 \cdot x\text{H}_2\text{O}$, > 99 wt. %), sodium aluminate (NaAlO_2 , Al_2O_3 wt. % = 55), tetrapropyl ammonium bromide (TPABr, $\text{C}_{12}\text{H}_{28}\text{BrN}$, >99 wt. %), ammonium nitrate (NH_4NO_3 , 99 wt. %), sodium hydroxide (NaOH, 99.6 wt. %) and sulfuric acid (H_2SO_4 , 98 wt. %) were purchased from Merck company (Germany).

Nanocatalyst preparation

High silica H-ZSM-5 zeolite catalyst (Si/Al=200) was synthesized by hydrothermal technique. A solution containing NaOH (5.58 g), sodium aluminate (0.46 g) and deionized water (66 cm^3) was stirred for 30 min. TPABr (13 g) was then added and stirred for 1

h (solution A). Simultaneously, silicic acid (67 g) was dissolved in 100 cm³ of deionized water (solution B). The solution A was added to the solution B drop by drop under continuous agitation and stirred for 2 h. An appropriate amount of sulfuric acid (H₂SO₄, 98 %, Merck) was used to adjust the pH of solution (10.5). The final solution included the molar composition of 20SiO₂: 0.05Al₂O₃: 1TPABr: 1.5Na₂O: 200H₂O. The crystallization was carried out in a static stainless-steel autoclave at 180°C under autogenous pressure for 48 h. The synthesized powder was filtered, washed, dried at 110°C overnight and then calcined at 540°C for 24 h (3°C/min) in air. The H-form ZSM-5 was prepared by four times ion-exchange with using 1M NH₄NO₃ (99 wt. %, Merck) solution for 10 h at 90°C under continuous agitation, followed by calcination at 540°C for 12 h (3°C/min) in air. The parent nanocatalyst was denoted as PZ.

Hierarchical nanocatalysts were prepared from calcined ZSM-5 zeolite. The treatment was done in 0.3 M aqueous solution of NaOH at 65°C for different durations (30 and 60 min). The modified solid was filtered, washed and dried at 110°C for 12 h. The H-form of powder was prepared by ion-exchange with a 1M NH₄NO₃ (99 wt. %, Merck) solution for 10 h at 90°C under continuous agitation, followed by calcination at 540°C for 12 h (3°C/min) in air. The prepared hierarchical nanocatalysts were denoted as DSZ_x, where x is the time of desilication process.

Characterization techniques

X-ray diffraction (XRD) experiments were carried out with a D8 Advance Bruker AXS X-ray diffractometer with Ni-filtered Cu K α radiation ($\lambda=0.15418$ nm) and 2θ variations in the range of 4-50° at 40 kV. A KYKY (Model, EM3200) equipment determined field-emission scanning electron microscopy (FE-SEM) images at a potential difference of 26 kV. Temperature-programmed desorption of ammonia (NH₃-TPD, Micromeritics, USA) with an on-line TCD detector characterized acidity. 53.6 mg of each sample was pretreated at 550°C for 4 h. The powders were saturated with NH₃ for 1 h in the micro reactor and helium flow passed over the sample with a heating rate of 10°C min⁻¹. The range of desorption temperature was 100-700°C. N₂ adsorption-desorption technique at -196.2°C (Quantachrome, USA) analyzed textural properties. The powders were degassed at 300°C for 3 h and then Brunauer-Emmet-Teller (BET) surface

area was measured. The total surface area (S_{BET}) and total pore volume (V_{total}) were determined using the BET isothermal equation and the nitrogen adsorbed volume at P/P₀ = 0.99, respectively. The t-plot method provides the micropore volume (V_{micro}). The mesopore volume (V_{meso}) is difference of the calculated total data and the corresponding micropore data. FTIR measurements were in a Nexus model infrared spectrophotometer (Nicolet Co, USA) at the resolution of 4 cm⁻¹. The samples were prepared as self-supported wafers containing 1 wt. % of the powder in KBr.

Catalyst testing

Methanol was converted to olefins over the nanocatalysts in a fixed-bed continuous-flow reactor set-up including a stainless steel tube reactor (450 mm length, 11 mm ID) [24]. A temperature-controlled three-zone furnace provided a constant temperature to the entire reactor. A K-type thermocouple probe near the nanocatalyst bed monitored the operational temperature. The operational condition was set as 480°C, atmospheric pressure and methanol weight hourly space velocity (WHSV) of 0.9 h⁻¹. The nano catalysts were stabled, crushed and sieved to get 16-25 mesh particle size for the experiments. The nanocatalysts loading was 4 g and a HPLC infusion pump supplied the feed (methanol/water = 1 wt. /wt.). The activation of nanocatalysts was examined in-situ at 300°C for 2 h (heating rate of 3°C min⁻¹) under N₂ flow. A heat-traced tube (120°C) was applied to avoid hydrocarbon condensation through the transfer line between the reactor and separator vessel. A micro gas chromatograph (Varian CP-4900) equipped with a TCD detector analyzed the up-stream of separator vessel (gas phase). The bottom stream in both aqueous and organic parts was separated. An off-line gas chromatograph (Varian CP-3800) equipped with TCD and FID detectors characterized the aqueous part. The organic part was analyzed by the off-line gas chromatograph (Varian CP-3800) equipped with an FID detector.

RESULTS AND DISCUSSION

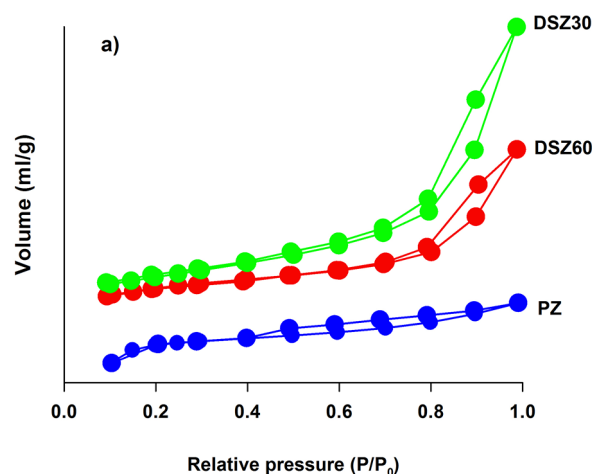
Structural and textural parameters of nanocatalysts

XRD patterns confirm that the resulting hierarchical nanocatalysts include the zeolite structure and the ap-

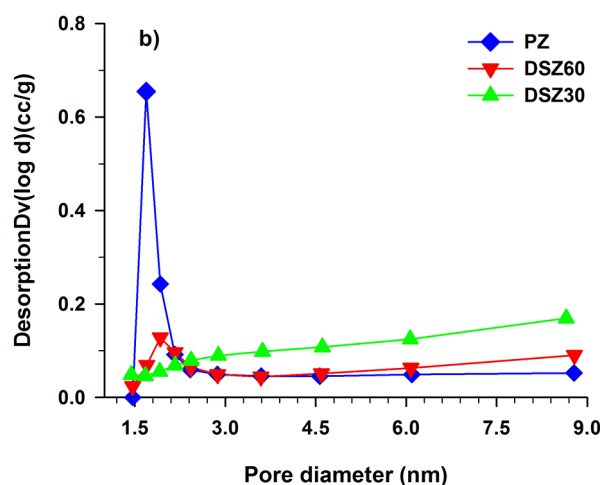
plied desilication have not changed the structure significantly. The relative crystallinity is the ratio of the large peak area found at $2\theta=22.5-25^\circ$ to that of the parent nanocatalyst. The alkali treatment decreases the relative crystallinity from 100 % to 82 % (Table 1) due to the slightly destruction of zeolite framework during Si extraction [25]. The microporous and mesoporous structures of nanocatalysts lead to the common Langmuir isotherms including types I and IV (Figure 1). Capillary condensation in mesoporous structures occurs at the high relative pressure of adsorbate. The mesoporosity in the alkali-treated ZSM-5 nanocatalysts includes both inter- and intraparticle mesopores. The isotherms represent a hysteresis loop in N_2 adsorption-desorption of the nanocatalysts as result of intraparticle mesopores (Figure 1). The isotherms show a sub-step in the low relative pressure ($P/P_0=0.1-0.2$) due to fluid-to-crystalline like phase transition of the adsorbed nitrogen [26]. This common phenomenon does not indicate the additional mesopore formation [27]. It worth to note that the isotherms of treated nanocatalysts show a sharp increasing in the high relative pressure ($P/P_0=1$). It reveals the interparticle mesopores formation between the ZSM-5 zeolite particles. The crystal agglomeration results in mesoporous structure in the form of interparticle spaces which is different from the intraparticle mesopores.

The pore size distribution of nanocatalysts confirms the formation of mesopores in the structures (Figure 1). The broad maximum in diameter shifts from ca. 1.70 nm to ca. 2.2 nm for the DSZ30 nanocatalyst. The DSZ60 nanocatalyst includes mesopores with a broad pore size distribution (2-10 nm) as a result of the high treatment temperature (65°C) and the longer treatment duration (60 min). Groen et al. [20] reported that the mesopore size can be adjusted by temperature and time of alkali treatment. The calculated textural data reveal the high surface area and mesopore volume of treated nanocatalysts (Table 1). The surface area reduction can be explained by the zeolite framework destroying owing to Si extraction and extra-framework formation through desilication.

Long-time desilication (DSZ60) extracts more Si



(a)



(b)

Figure 1. N_2 adsorption-desorption isotherms and BJH pore size distribution of the nanocatalysts.

which leads to more reduction in the crystallinity. The results are in consistent with the XRD results. You et al. [25] studied desilication of ZSM-5 catalyst ($\text{Si}/\text{Al}=12$) using 0.2-0.6 M aqueous solution of NaOH at 65°C for 2 h. They found that framework Al (FAL) content decreased significantly through the harsh desilication (0.4 M NaOH solution) owing to the formation of more extra framework Al (EFAL) content. Furthermore, long-time desilication favored the mesopore volume formation but decreased the micropore volume.

Table 1. Crystallinity and textural data.

Sample	Crystallinity (%)	S_{BET} (m^2g^{-1})	V_{total} (cm^3g^{-1})	V_{micro} (cm^3g^{-1})	V_{meso} (cm^3g^{-1})
PZ	100.00	263.30	0.16	0.10	0.06
DSZ30	88.14	161.90	0.23	0.02	0.21
DSZ60	82.45	189.50	0.36	0.01	0.35

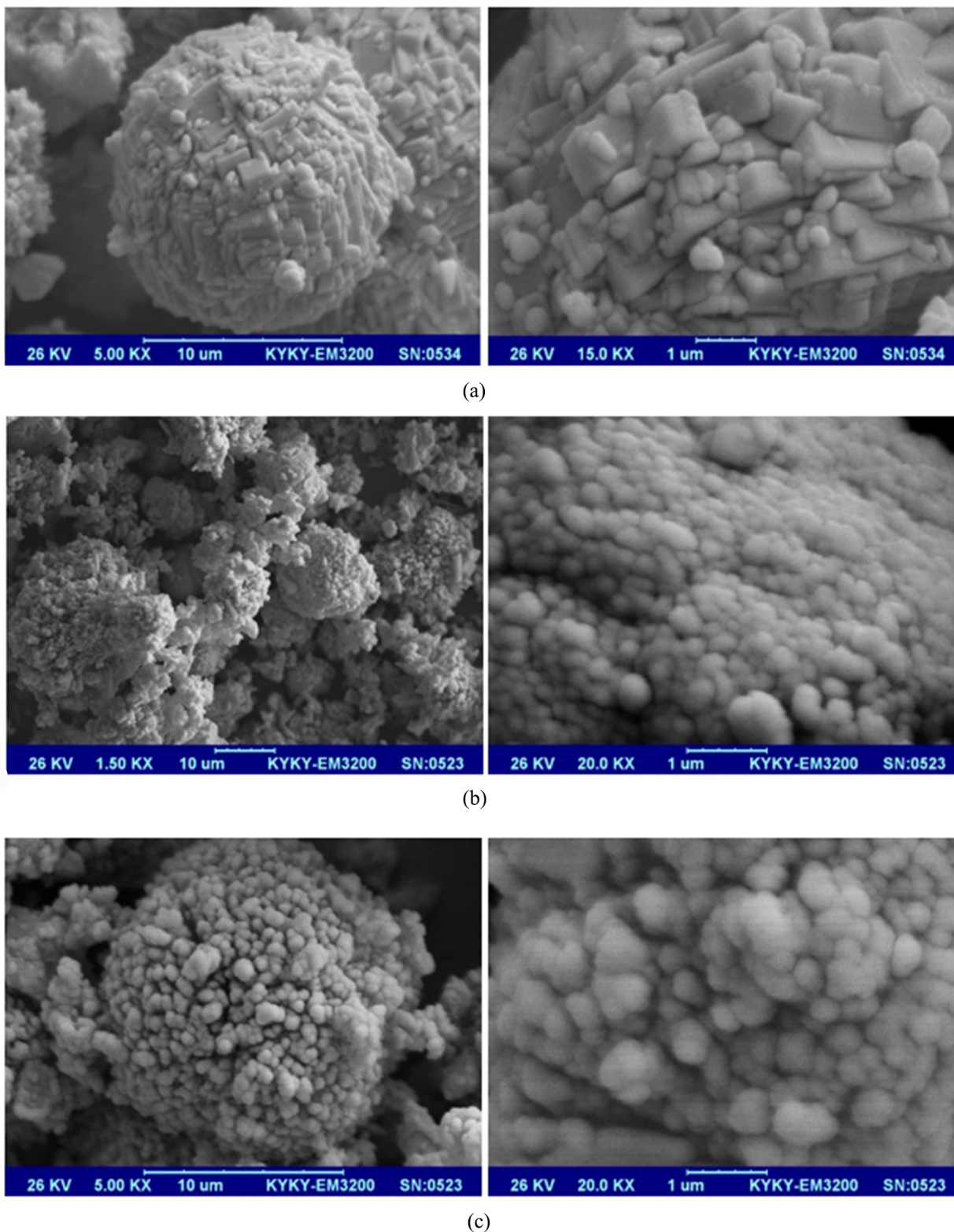


Figure 2. FE-SEM images of the nanocatalysts (a) PZ; (b) DSZ60; (c) DSZ30.

FE-SEM images show relatively uniform surface morphology (Figure 2). The nanocatalysts are in the form of spherical aggregation. TEM images of individual microsphere surface confirmed that nanosized crystals aggregation formed the microspheres [28, 29]. It

worth noting that the applied desilication process does not destroy morphology which agrees with the XRD results. The surface of nanocatalysts becomes rough after treatment and the edges of ZSM-5 particles have been melted and taken spherical shape. The results are

in agreement with literature [30, 31].

FTIR analysis of nanocatalysts

FTIR spectra of the nanocatalysts were recorded in the range of 400-4000 cm^{-1} . Internal SiO_4 and AlO_4 tetrahedral lead to the band near ca. 450 cm^{-1} (Figure 3a). The band around ca. 550 cm^{-1} indicates the ZSM-5 zeolite with five membered rings. The adsorptions at ca. 800 cm^{-1} and ca. 1100 cm^{-1} can attribute to the symmetric stretching of external and internal linkages, respectively. The existence of structures with four chains of 5-rings results in the band at ca. 1225 cm^{-1} . FTIR spectra in the range of 3500-3800 cm^{-1} can be used to investigate surface hydroxyl (OH) groups (Figure 3b). The band at ca. 3610 cm^{-1} is assigned to the vibration of bridging Si-OH-Al groups [32, 33].

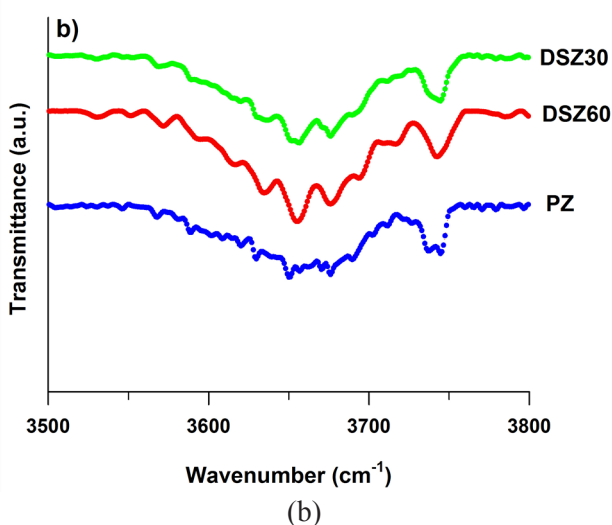
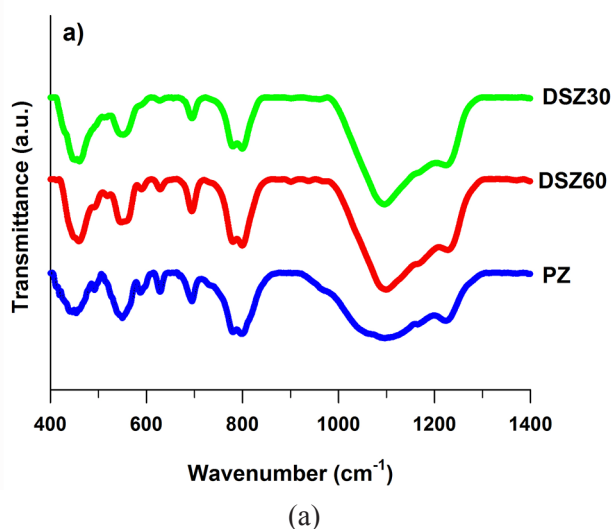


Figure 3. FTIR spectra of the nanocatalysts in the range of (a) 400-1400 cm^{-1} ; (b) 3500-3800 cm^{-1} .

The intensity of 3610 cm^{-1} band increases through the alkali treatment. This phenomenon can be explained by the selective Si atom extraction and formation of the Si(OH)Al groups [34]. The band at 3680 cm^{-1} characterizes EFAl species (Al-OH) in the nanocatalysts [35]. The band at ca. 3750 cm^{-1} can be assigned to the vibrations of the isolated Si-OH silanols located on the external surface or mesopores surface [8]. The intensity of 3750 cm^{-1} band for the DSZ60 nanocatalyst is higher than that for the parent nanocatalyst which reveals the secondary mesopores generation and supports the N_2 adsorption-desorption results.

NH_3 -TPD analysis of nanocatalysts

The parent and DSZ30 nanocatalysts represent similar NH_3 -TPD pattern including different strength and amount of the acid sites (Figure 4). According to the method of Ramirez [36], the relative concentrations of weak (100-200 $^{\circ}\text{C}$), medium (200-300 $^{\circ}\text{C}$) and strong (>300 $^{\circ}\text{C}$) acid sites were determined (Table 2). Alkali treatment decreases the percentage of strong acid sites while increases the weak and medium acidity. Desilication for the long time removes the strong acid sites and thereby the DSZ60 nanocatalyst represents no peak in the high temperature range. You et al. [25] found that alkali treatment of H-ZSM-5 zeolite with NaOH solutions (0.2 and 0.4 M at 65 $^{\circ}\text{C}$ for 2 h) eliminated the strong acid sites and increased the strength and concentration of weak acid sites.

Tarach et al. [21] reported that desilication process resulted in the formation of acid sites which were located individually inside micropores. The maximum

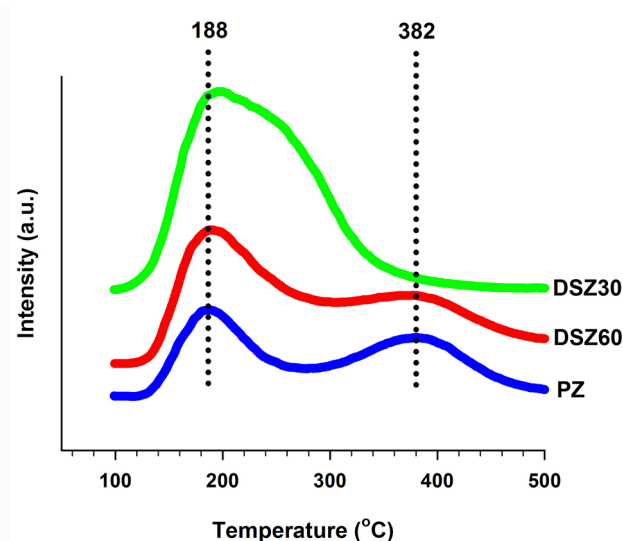


Figure 4. NH_3 -TPD profiles of the nanocatalysts.

Table 2. Acidity of the nanocatalysts.

Sample	Acidity (mmol NH ₃ g ⁻¹)		
	PZ	DSZ30	DSZ60
Weak	0.17 (24 %)	0.27 (24 %)	0.64 (31 %)
Medium	0.20 (28 %)	0.42 (37 %)	1.25 (61 %)
Strong	0.34 (48 %)	0.44 (39 %)	0.16 (8 %)
Total	0.71	1.13	2.05

temperature of peaks shifts toward the higher temperatures which indicates the higher strength of acid sites for the treated nanocatalysts compared with the parent nanocatalyst. The results are in consistent with literature [37-39].

It worth mentioning that the concentration of strong and weak acid sites attribute to Si and Al content in zeolite framework, respectively. The strength of acidity is in the order of Al>>Si [40, 41]. Consequently, the preferential removing of framework Si and the increased Al concentration by formation of more Al-OH groups result in the high strength and concentration of weak acid sites in the alkali-treated nanocatalysts. The weak acid sites assigned to EFAl and the strong acid sites depend on the -OH groups of FAI[42, 43]. The NH₃-TPD results support the FTIR results.

Catalytic test in MTO reaction

Methanol dehydration is an acid-catalyzed reaction which provides wide range of hydrocarbons. The MTO reaction was carried out in a fixed bed reactor over the parent and hierarchical nanocatalysts. The operational conditions were 480°C, atmospheric pressure, methanol WHSV of 0.9 h⁻¹ and 50 wt. % methanol in water solution as feed. The high methanol conversion (100 %) was obtained over the nanocatalysts for the long time on stream. Both acidic properties and accessibility of acid sites to the molecules of reagent influence the catalytic activity of the nanocatalysts. It is well accepted that the framework structure, pore architecture and acidity of zeolite catalysts control their performance in the MTO reaction [44-46].

Based on the hydrocarbon pool mechanism, the MTO reaction includes the following three main steps: i) methanol dehydration and dimethyl ether (DME) formation, ii) the initial C-C bond formation, and iii) higher production of hydrocarbons from the primary products.

The weak acid sites carry out methanol to DME conversion [24, 47] as well as alkylation and methylation reactions [48]. The strong acid sites initiate C-C bond generation and also coke formation in the

MTO reaction [35, 49]. Therefore, the strong acidity of catalyst leads to the shorter catalytic lifetime due to the fast deactivation. The high surface area and mesopore volume facilitate the component diffusion out of the pores and decrease the diffusion resistance which hinder pore blocking by coke deposition. In this regards, the DSZ60 nanocatalyst represents the highest propylene selectivity (ca. 43 %) in the MTO reaction (Figure 5). The prolonged treatment (60 min) at alkaline solution results in the high surface area (189.5 m² g⁻¹) and high mesopore volume (0.35 cm³ g⁻¹). The mesopore formation is beneficial for the more accessibility of surface acid sites to the reactants. The acidity of catalyst is a crucial parameter for catalytic activity through the MTO reaction [47, 50]. The variation of acid sites influences product distribution and rate of deactivation. The weak and medium acid sites enhance propylene production through the alkylation and methylation reactions. The strong acid sites are the main active sites for the conversion of light olefins to paraffins, aromatics, naphthenes and higher olefins. The medium acidity results in more light olefins, less low-value hydrocarbons, less coke formation and long catalytic lifetime [51-53]. Therefore, the high concentration of weak and medium acid sites for the DSZ60 nanocatalyst supports the high propylene selectivity.

The higher concentration and strength of strong acid sites compared with the parent nanocatalyst lead to the high rate of alkene methylation reactions over the DSZ30 nanocatalyst which produces more heavy hydrocarbons (C₅₊). Sevell et al. [54] considered trimethylbenzene (triMB) as main hydrocarbon pool interme-

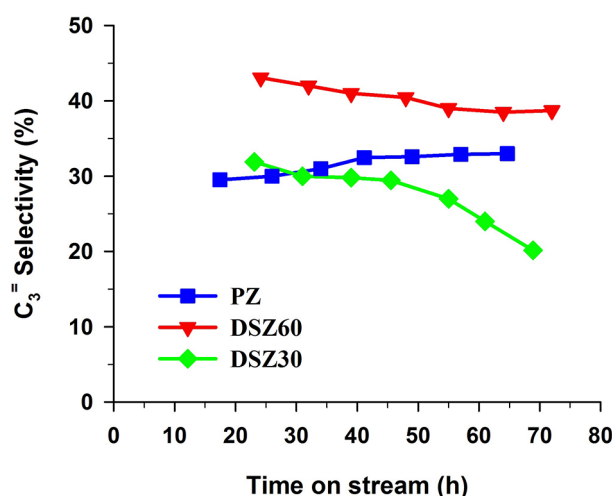


Figure 5. Propylene selectivity over the nanocatalysts with time on stream (reaction conditions: T=480°C, WHSV=0.9 h⁻¹, P=1 atm, methanol/water 1:1 by weight).

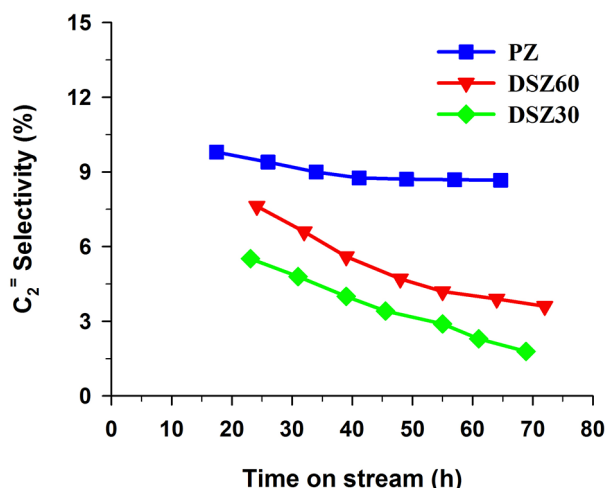


Figure 6. Ethylene selectivity over the nanocatalysts with time on stream (reaction conditions: $T=480^{\circ}\text{C}$, $\text{WHSV}=0.9\text{ h}^{-1}$, $P=1\text{ atm}$, methanol/water 1:1 by weight).

diates for the MTO reaction over the H-ZSM-5 catalyst. They found that the MTO reaction occurred through a dual-cycle mechanism. Ethylene and toluene are the products of triMB cracking (cycle I), while alkene methylation and cracking reactions produce propylene and higher olefins (cycle II). The results show that the small pore dimension forces the hydrocarbon pool via smaller aromatics intermediates which favors ethylene production. Consequently, compared with the pore size of the parent nanocatalyst, the large pore size of alkaline-treated nanocatalysts leads to low ethylene selectivity (Figure 6). Deactivation of strong acid sites with time on stream decreases the triMB cracking rate as well as the rate of ethylene production. As a result, the drop in the ethylene selectivity with time on stream over the nanocatalysts is in agreement with the dual-cycle mechanism.

The methylation of light olefins produces butene through the MTO reaction [54]. Wu et al. [55] found that $\text{C}_4^=$ oligomerization produced $\text{C}_8^=$ olefin. In general, butene selectivity decreases over the alkali-treated nanocatalysts (Figure 7). This phenomenon can be explained by the catalyst deactivation which reduces cracking rate. Increasing trend of $\text{C}_4^=$ selectivity

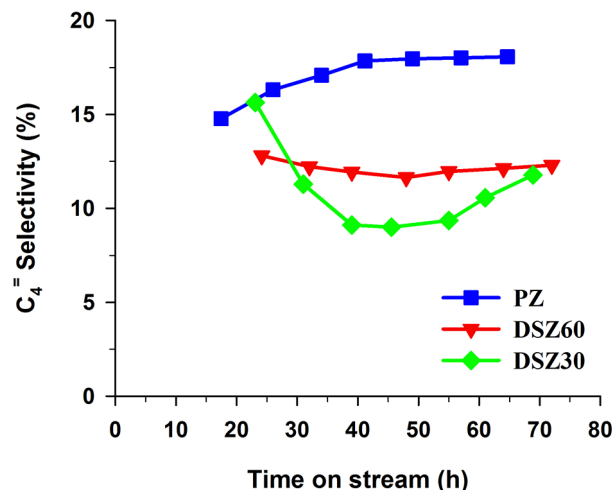


Figure 7. Butene selectivity over the nanocatalysts with time on stream (reaction conditions: $T=480^{\circ}\text{C}$, $\text{WHSV}=0.9\text{ h}^{-1}$, $P=1\text{ atm}$, methanol/water 1:1 by weight).

over the PZ nanocatalyst can be attributed to the low strength of strong acid sites and thereby the low rate of $\text{C}_4^=$ oligomerization. The high butene selectivity at the end of time on stream over the DSZ60 nanocatalyst indicates the fast deactivation of nanocatalyst. C_4 hydrogen transfer index (HTI) reveals the progress of hydrogen transfer reactions over the nanocatalyst [56]. C_4 HTI is the ratio of butane yield (iso- C_4 and n- C_4) to the total C_4 hydrocarbons yield (alkanes and alkenes). The nanocatalysts represent decreasing trend of C_4 HTI (Figure 8) because coke formation reduces the acid sites density as well as the rate of hydrogen transfer and cyclization reactions.

The high C_4 HTI of DSZ60 nanocatalyst is in consistent with the overall decreasing trend of $\text{C}_4^=$ selectivity. The high weak and medium acidity of DSZ60 nanocatalyst promotes butene consumption by methylation reaction. The prolonged alkali treatment (DSZ60) generates more mesopore structures which leads to the high heavy hydrocarbons selectivity (Table 3). The high mesopore volume accelerates olefins desorption. The large pore size is beneficial for the easy exit of heavy hydrocarbons and the low rate of coke formation.

Table 3. Average heavy hydrocarbons selectivity for the nanocatalysts.

Characteristic	Selectivity (%)						
	C_5	C_6	C_7	C_8	C_9	C_{10+}	Total
PZ	3.56	7.46	0.87	1.60	0.68	0.20	14.37
DSZ30	4.28	11.18	1.48	3.37	2.98	1.29	24.58
DSZ60	5.08	13.57	1.98	3.19	2.47	0.58	26.87

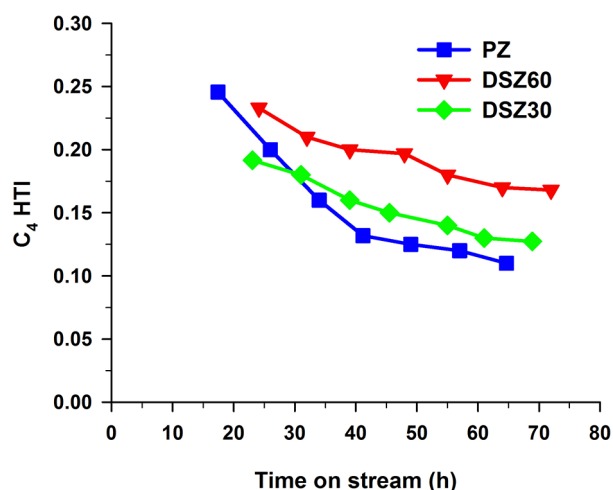


Figure 8. C₄-HTI for the nanocatalysts with time on stream (reaction conditions: T=480°C, WHSV=0.9 h⁻¹, P=1 atm, methanol/water 1:1 by weight).

The nanocatalysts represent a similar trend for the light paraffins (C₁-C₄) selectivity (Figure 9). Catalyst deactivation decreases the selectivity with time on stream. Coke formation blocks the pores and does not allow the methanol molecules to access to the acid sites. Hence, more methanol molecules are adsorbed on the basic sites and decomposed to CO, CO₂ and CH₄ components. The parent nanocatalyst produces less aromatics and more paraffins, which agree with the low mesopore volume and high strong acidity. The low light paraffins selectivity over the hierarchical nanocatalysts (< 6 %) confirms their stable performance. The large pore size suppresses the coke deposition and catalyst deactivation. Furthermore, the high

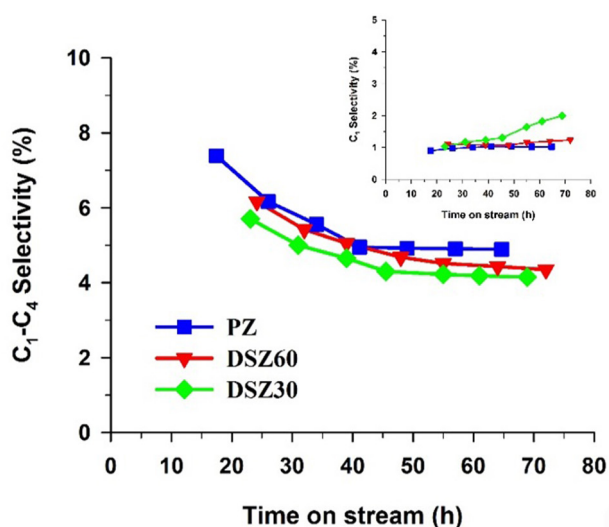


Figure 9. Light paraffins selectivity over the nanocatalysts with time on stream (reaction conditions: T=480°C, WHSV=0.9 h⁻¹, P=1 atm, methanol/water 1:1 by weight).

mesopore volume increases the access of methanol molecules to the internal acid sites.

CONCLUSION

High silica hierarchical H-ZSM-5 nanocatalysts have prepared and characterized for the MTO reaction. The appropriate desilication process extracted Si species with no change in the structure of parent nanocatalyst. Alkali treatment increased the mesoporosity and medium acidity by more than five and two folds, respectively. Consequently, the developed hierarchical nanocatalyst represented the high propylene selectivity for the long catalytic lifetime. The reported desilication process is an excellent post treatment for the high silica H-ZSM-5 nanocatalyst which enhances its catalytic activity under conditions relevant to the industrial MTO process. The results could improve the comparability of the MTO process with the conventional processes for production of light olefins.

ACKNOWLEDGEMENTS

The authors also wish to acknowledge the support of the Sahand University of Technology and the Petrochemical Research and Technology Company of the National Petrochemical Company for this study.

REFERENCES

1. Tian P, Wei Y, Ye M, Liu Z (2015) Methanol to olefins (MTO): From fundamentals to commercialization. *ACS Catalysis* 5: 1922-1938
2. Xiang D, Yang S, Qian Y (2016) Techno-economic analysis and comparison of coal based olefins processes. *Energy Conv Manage* 110: 33-41
3. Yazdani M, Haghighi M, Ashkriz S (2016) Mixing-assisted hydrothermal synthesis of nanostructured ZnAPSO-34 used in conversion of methanol to light olefins: Effect of agitation RPM on catalytic properties and performance. *Asia-Pacific J Chem Eng* 11: 766-777
4. Kaarsholm M, Joensen F, Nerlov J, Cenni R, Chaouki J, Patience GS (2007) Phosphorous modified ZSM-5: Deactivation and product distribution for MTO. *Chem Eng Sci* 62: 5527-5532

5. Aghaei E, Haghghi M (2015) Effect of crystallization time on properties and catalytic performance of nanostructured SAPO-34 molecular sieve synthesized at high temperatures for conversion of methanol to light olefins. *Powder Technol* 269: 358-370
6. Rostamizadeh M, Boffito DC, Patience GS, Taeb A (2014) Neural network modeling of methanol to propylene over P-ZSM-5 in a fluidized bed. *J Chem Proc Engg* 1: 1-8
7. Wang Q, Wang L, Wang H, Li Z, Wu H, Li G, Zhang X, Zhang S (2011) Synthesis, characterization and catalytic performance of SAPO-34 molecular sieves for methanol-to-olefin (MTO) reaction. *Asia-Pacific J Chem Eng* 6: 596-605
8. Kanyi C (2016) Mesoporous zeolites: Preparation, characterization and applications. *Johnson Matthey Technol Rev* 60: 25-28
9. Ahmadpour J, Taghizadeh M (2015) Catalytic conversion of methanol to propylene over high-silica mesoporous ZSM-5 zeolites prepared by different combinations of mesogenous templates. *J Natural Gas Sci Eng* 23: 184-194
10. Ahmadpour J, Taghizadeh M (2015) Selective production of propylene from methanol over high-silica mesoporous ZSM-5 zeolites treated with NaOH and NaOH/tetrapropylammonium hydroxide. *Comptes Rendus Chimie* 18: 834-847
11. Song C-M, Yan Z-F (2008) Synthesis and characterization of M-ZSM-5 composites prepared from ZSM-5 zeolite. *Asia-Pacific J Chem Eng* 3: 275-283
12. Fathi S, Sohrabi M, Falamaki C (2014) Improvement of HZSM-5 performance by alkaline treatments: Comparative catalytic study in the MTG reactions. *Fuel* 116: 529-537
13. Ahn JH, Kolvenbach R, Neudeck C, Al-Khattaf SS, Jentys A, Lercher JA (2014) Tailoring mesoscopically structured H-ZSM5 zeolites for toluene methylation. *J Catal* 311: 271-280
14. He Y, Liu M, Dai C, Xu S, Wei Y, Liu Z, Guo X (2013) Modification of nanocrystalline HZSM-5 zeolite with tetrapropylammonium hydroxide and its catalytic performance in methanol to gasoline reaction. *Chinese J Catal* 34: 1148-1158
15. Ghavipour M, Behbahani RM, Moradi GR, Soleimanimehr A (2013) Methanol dehydration over alkali-modified H-ZSM-5; Effect of temperature and water dilution on products distribution. *Fuel* 113: 310-317
16. Bleken FL, Barbera K, Bonino F, Olsbye U, Lillerud KP, Bordiga S, Beato P, Janssens TVW, Svelle S (2013) Catalyst deactivation by coke formation in microporous and desilicated zeolite H-ZSM-5 during the conversion of methanol to hydrocarbons. *J Catal* 307: 62-73
17. Kim J, Choi M, Ryoo R (2010) Effect of mesoporosity against the deactivation of MFI zeolite catalyst during the methanol-to-hydrocarbon conversion process. *J Catal* 269: 219-228
18. Mochizuki H, Yokoi T, Imai H, Namba S, Kondo JN, Tatsumi T (2012) Effect of desilication of H-ZSM-5 by alkali treatment on catalytic performance in hexane cracking. *Appl Catal A-General* 449: 188-197
19. Schmidt F, Lohe MR, Büchner B, Giordanino F, Bonino F, Kaskel S (2013) Improved catalytic performance of hierarchical ZSM-5 synthesized by desilication with surfactants. *Micropor Mesopor Mater* 165: 148-157
20. Groen JC, Peffer LAA, Moulijn JA, Pérez-Ramírez J (2004) Mesoporosity development in ZSM-5 zeolite upon optimized desilication conditions in alkaline medium. *Colloid Surface A* 241: 53-58
21. Tarach KA, Martínez-Triguero J, Rey F, Góra-Marek K (2016) Hydrothermal stability and catalytic performance of desilicated highly siliceous zeolites ZSM-5. *J Catal* 339: 256-269
22. Rostamizadeh M, Taeb A (2015) Highly selective Me-ZSM-5 catalyst for methanol to propylene (MTP). *J Ind Eng Chem* 27: 297-306
23. Hadi N, Niaei A, Nabavi SR, Alizadeh R, Shirazi MN, Izadkhah B (2015) An intelligent approach to design and optimization of M-Mn/H-ZSM-5 (M: Ce, Cr, Fe, Ni) catalysts in conversion of methanol to propylene. *J Taiwan Ins Chem Eng* 59: 173-185
24. Rostamizadeh M, Yaripour F (2017) Dealumination of high silica H-ZSM-5 as long-lived nanocatalyst for methanol to olefin conversion. *J Taiwan Ins Chem Eng* 71: 454-463
25. You SJ, Park ED (2014) Effects of dealumination and desilication of H-ZSM-5 on xylose dehydration. *Micropor Mesopor Mater* 186: 121-129
26. Groen JC, Peffer LA, Moulijn JA, Pérez-Ramírez

- J (2005) Mechanism of hierarchical porosity development in MFI zeolites by desilication: The role of aluminium as a pore-directing agent. *Chemistry* 11: 4983-4994
27. Hu Z, Zhang H, Wang L, Zhang H, Zhang Y, Xu H, Shen W, Tang Y (2014) Highly stable boron-modified hierarchical nanocrystalline ZSM-5 zeolite for the methanol to propylene reaction. *Catal Sci Technol* 4: 2891-2895
28. Chen L, Zhu SY, Wang YM, He M-Y (2010) One-step synthesis of hierarchical pentasil zeolite microspheres using diamine with linear carbon chain as single template. *New J Chem* 34: 2328-2334
29. Rostamizadeh M, Yaripour F (2016) Bifunctional and bimetallic Fe/ZSM-5 nanocatalysts for methanol to olefin reaction. *Fuel* 181: 537-546
30. Gao X, Tang Z, Lu G, Cao G, Li D, Tan Z (2010) Butene catalytic cracking to ethylene and propylene on mesoporous ZSM-5 by desilication. *Solid State Sci* 12: 1278-1282
31. Xin H, Li X, Fang Y, Yi X, Hu W, Chu Y, Zhang F, Zheng A, Zhang H, Li X (2014) Catalytic dehydration of ethanol over post-treated ZSM-5 zeolites. *J Catal* 312: 204-215
32. Gil B, Mokrzycki Ł, Sulikowski B, Olejniczak Z, Walas S (2010) Desilication of ZSM-5 and ZSM-12 zeolites: Impact on textural, acidic and catalytic properties. *Catal Today* 152: 24-32
33. O'Malley AJ, Parker SF, Chutia A, Farrow MR, Silverwood IP, Garcia-Sakai V, Catlow CRA (2016) Room temperature methoxylation in zeolites: Insight into a key step of the methanol-to-hydrocarbons process. *Chem Commun* 52: 2897-2900
34. Sadowska K, Wach A, Olejniczak Z, Kuśtrowski P, Datka J (2013) Hierarchic zeolites: Zeolite ZSM-5 desilicated with NaOH and NaOH/tetrabutylamine hydroxide. *Micropor Mesopor Mater* 167: 82-88
35. Campbell SM, Jiang X-Z, Howe RF (1999) Methanol to hydrocarbons: Spectroscopic studies and the significance of extra-framework aluminium. *Micropor Mesopor Mater* 29: 91-108
36. Ramírez J, Contreras R, Castillo P, Klimova T, Zárate R, Luna R (2000) Characterization and catalytic activity of CoMo HDS catalysts supported on alumina-MCM-41. *Appl Catal A-General* 197: 69-78
37. Zhang L, Qu S, Wang L, Zhang X, Liu G (2013) Preparation and performance of hierarchical HZSM-5 coatings on stainless-steel microchannels for catalytic cracking of hydrocarbons. *Catal Today* 216: 64-70
38. Zhou J, Teng J, Ren L, Wang Y, Liu Z, Liu W, Yang W, Xie Z (2016) Full-crystalline hierarchical monolithic ZSM-5 zeolites as superiorly active and long-lived practical catalysts in methanol-to-hydrocarbons reaction. *J Catal* 340: 166-176
39. Lai P-C, Chen C-H, Hsu H-Y, Lee C-H, Lin Y-C (2016) Methanol aromatization over Ga-doped desilicated HZSM-5. *RSC Advances* 6: 67361-67371
40. Kawase R, Iida A, Kubota Y, Komura K, Sugi Y, Oyama K, Itoh H (2007) Hydrothermal synthesis of calcium and boron containing MFI-Type zeolites by using organic amine as structure directing agent. *Ind Eng Chem Res* 46: 1091-1098
41. Chae H-J, Song Y-H, Jeong K-E, Kim C-U, Jeong S-Y (2010) Physicochemical characteristics of ZSM-5/SAPO-34 composite catalyst for MTO reaction. *J Phys Chem Solids* 71: 600-603
42. Triantafillidis CS, Vlessidis AG, Nalbandian L, Evmiridis NP (2001) Effect of the degree and type of the dealumination method on the structural, compositional and acidic characteristics of H-ZSM-5 zeolites. *Micropor Mesopor Mater* 47: 369-388
43. Woolery GL, Kuehl GH, Timken HC, Chester AW, Vartuli JC (1997) On the nature of framework Brønsted and Lewis acid sites in ZSM-5. *Zeolites* 19: 288-296
44. Kaarsholm M, Rafii B, Joensen F, Cenni R, Chaouki J, Patience GS (2009) Kinetic modeling of methanol-to-olefin reaction over ZSM-5 in fluid bed. *Ind Eng Chem Res* 49: 29-38
45. Hadi N, Niaei A, Nabavi SR, Navaei Shirazi M, Alizadeh R (2015) Effect of second metal on the selectivity of Mn/H-ZSM-5 catalyst in methanol to propylene process. *J Ind Eng Chem* 29: 52-62
46. Ahmed S (2012) Methanol to olefins conversion over metal containing MFI-type zeolites. *J Porous Mater* 19: 111-117
47. Xu A, Ma H, Zhang H, Ying W, Fang D (2013) Effect of boron on ZSM-5 catalyst for methanol to propylene conversion. *Polish J Chem Technol* 15: 95-101
48. O'Malley AJ, Logsdail AJ, Sokol AA, Catlow

- CRA (2016) Modelling metal centres, acid sites and reaction mechanisms in microporous catalysts. *Faraday Discus* 188: 235-255
49. Rostamizadeh M, Taeb A (2016) Synthesis and characterization of HZSM-5 catalyst for methanol to propylene (MTP) reaction. *Synth React Inorg M* 46: 665-671
50. Aghaei E, Haghghi M (2015) High temperature synthesis of nanostructured Ce-SAPO-34 catalyst used in conversion of methanol to light olefins: Effect of temperature on physicochemical properties and catalytic performance. *J Porous Mater* 22: 187-200
51. Yaripour F, Shariatinia Z, Sahebdehfar S, Irandoukht A (2015) Effect of boron incorporation on the structure, products selectivities and lifetime of H-ZSM-5 nanocatalyst designed for application in methanol-to-olefins (MTO) reaction. *Micropor Mesopor Mater* 203: 41-53
52. Yaripour F, Shariatinia Z, Sahebdehfar S, Irandoukht A (2015) Conventional hydrothermal synthesis of nanostructured H-ZSM-5 catalysts using various templates for light olefins production from methanol. *J Natural Gas Sci Eng* 22: 260-269
53. Miar Alipour S, Halladj R, Askari S, BagheriSereshki E (2016) Low cost rapid route for hydrothermal synthesis of nano ZSM-5 with mixture of two, three and four structure directing agents. *J Porous Mater* 23: 145-155
54. Svelle S, Olsbye U, Joensen F, Bjørgen M (2007) Conversion of methanol to alkenes over medium- and large-pore acidic zeolites: Steric manipulation of the reaction intermediates governs the ethene/propene product selectivity. *J Phys Chem C* 111: 17981-17984
55. Wu W, Guo W, Xiao W, Luo M (2011) Dominant reaction pathway for methanol conversion to propene over high silicon H-ZSM-5. *Chem Eng Sci* 66: 4722-4732
56. Bjørgen M, Joensen F, Spangsberg Holm M, Olsbye U, Lillerud K-P, Svelle S (2008) Methanol to gasoline over zeolite H-ZSM-5: Improved catalyst performance by treatment with NaOH. *Appl Catal A-General* 345: 43-50